Biol. Cybern. 61, 379–392 (1989)

Biological Cybernetics

Modeling the Olfactory Bulb and its Neural Oscillatory Processings

Z. Li[1] and J. J. Hopfield[2]

[1] Division of Physics, Mathematics and Astronomy, and [2] Division of Biology, and Division of Chemistry and Chemical Engineering, AT & T Bell Laboratories, California Institute of Technology, Pasadena, Ca 91125, USA

Abstract. The olfactory bulb of mammals aids in the discrimination of odors. A mathematical model based on the bulbar anatomy and electrophysiology is described. Simulations of the highly non-linear model produce a 35–60 Hz modulated activity which is coherent across the bulb. The decision states (for the odor information) in this system can be thought of as stable cycles, rather than point stable states typical of simpler neuro-computing models. Analysis shows that a group of coupled non-linear oscillators are responsible for the oscillatory activities. The output oscillation pattern of the bulb is determined by the odor input. The model provides a framework in which to understand the transform between odor input and the bulbar output to olfactory cortex. There is significant correspondence between the model behavior and observed electrophysiology.

1 Introduction

The olfactory system is a phylogenetically primitive part of the cerebral cortex (Shepherd 1979). In lower vertebrates, the olfactory system is the largest part of the telencephalon. This system also has a simple cortical intrinsic structure, which in modified form is used in other parts of the brain (Shepherd 1979). The olfactory system deals with a relatively simple computational problem compared to vision or audition, since molecules of the distal object to be detected are bound to and crudely recognized by receptor proteins. Having phylogenetic importance and computational simplicity, the olfactory system is an ideal candidate to yield insight on the principles of sensory information processing.

The olfactory system includes the receptor cells within the nasal cavity, the olfactory bulb, and the olfactory cortex which receives the inputs from the olfactory bulb (Fig. 1). Odorant molecules selectively increase the firing rates of the spontaneously active receptor cells (Sicard and Holley 1984), whose axons carry the odor information to the olfactory bulb. The olfactory bulb also receives inputs from the olfactory cortex and the "diagonal band" (Shepherd 1979) at the base of the brain. Both the bulb and the prepiriform cortex to which it sends its efferents exhibit similar 35–90 Hz rhythmic population activity as seen in EEG recordings, modulated by breathing.

The anatomy and physiology of the olfactory bulb are well studied. Efforts have been made to model its information processing function (Freeman 1979b, c; Freeman and Schneider 1982; Freeman and Skarda 1985; Baird 1986; Skarda and Freeman 1987), which is still unclear (Scott 1986). The position of the bulb in the olfactory pathway makes it a likely location of information processing to increase the identifiability of odors. The linkage of the bulbar and cortical oscillatory activity with the sniff cycles suggests that the oscillation plays an important role in the olfactory information processing (Freeman and Skarda 1985; Baird 1986; Skarda and Freeman 1987). We will examine the way in which the bulbar oscillation pattern originates, and how this pattern, which can be thought of as the decision state about odor information, depends on the input odor.

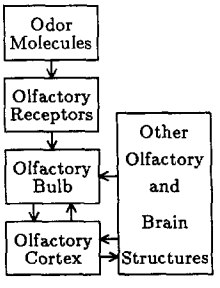

Fig. 1. Olfactory system and its environment

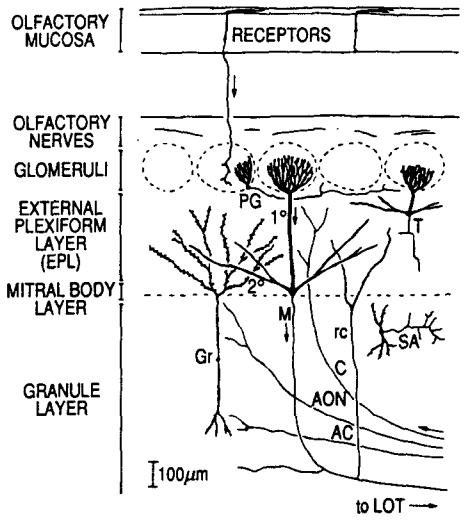

Fig. 2. Neuronal elements of the mammalian olfactory bulb. Inputs: olfactory nerves (above) from the receptors; central fibers (C, AON and AC) from the higher centers. Neurons: mitral cell (M), with primary (1°) and secondary dendrites (2°) and recurrent axon collaterals (rc); tufted cell (T), a smaller version of mitral cells; granule cell (Gr); inhibitory cell (PG) in the input layer; deep short axon cells (SA) which are small in number. Outputs: LOT to olfactory cortex. Taken from Shephard (1979)

2 Anatomical and Physiological Background

The olfactory bulb has clearly differentiated types of neurons located on different parallel lamina. These lamina lie on a surface which is roughly a segment of a sphere or ellipsoid. Each receptor sends a single unbranched axon to the topmost layer, terminating in one of the spherical regions of neuropil termed glomeruli (Fig. 2; Shepherd 1979). The receptor axons ramify inside it and synapse on the dendrites of the excitatory mitral cells and on dendrites of inhibitory short axon cells. The short axon cells make local dendrodendritic contacts with mitral cells. A few axons from the diagonal band also synapse on the mitral dendrites in this layer (Shepherd 1979).

The main cell types of the bulb are the (excitatory) mitral cells, whose cell bodies lie below the input layer, and the (inhibitory) granule cells lying deep below the layer of mitral cell bodies (Shepherd 1979). Each mitral cell sends an unbranched primary dendrite to one glomerulus. The granule cell upper dendrites receive excitation from the mitral cell secondary dendrites and send inhibition back to them by local dendrodendritic interaction on their dendritic connections. Most of these dendrodendritic connections are reciprocal and extend locally to other cells within a few hundred microns, the space below several glomeruli (Shepherd 1979) in the input layer. The mitral cell axons also send collaterals to the local granule cell lower dendrites. The granule cells do not have a morphological axon. While

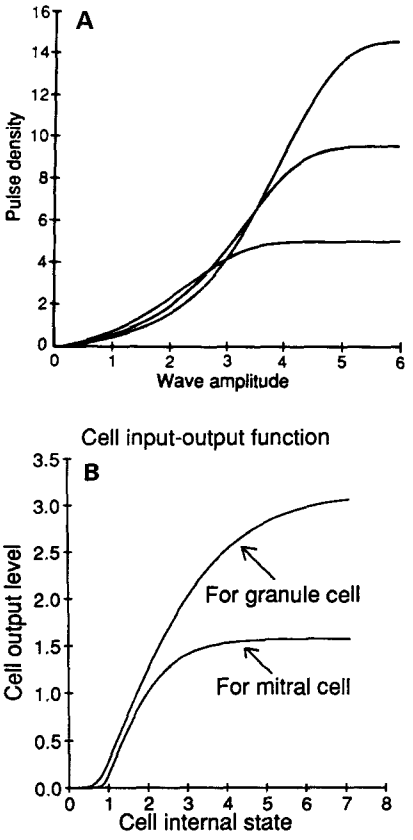

Fig. 3A and B. Cell non-linear input-output functions. **A** Three examples of experimentally measured functions in a mass of mitral and granule cells, relating the pulse probability of single or small groups of mitral cells to the EEG wave amplitude originated from the granule cells. Taken from Freeman and Skarda (1985). **B** The model functions for mitral and granule cells respectively

they can produce action potentials (Mori and Kishi 1982), their outputs are dominantly via granule-to-mitral dendrodendritic synapses activated by graded presynaptic depolarization (Shepherd 1979; Jahr and Nicoll 1980). There are also smaller excitatory cells called tufted cells, and inhibitory interneural short axon cells which are very few compared with the interneural granule cells.

Most inputs from higher olfactory centers and other parts of the brain are directed to the dendrites of the granule cells. The outputs of the bulb are carried by the mitral cell axons. There are ~1000 receptor axons and dendrites from 25 mitral cells in each glomerulus, while there are ~200 granule cells for each mitral cell. A rabbit has about 50,000 mitral cells (Shepherd 1979). Both the mitral and granule cells have a non-linear input-output relationship, which can be qualitatively seen in physiological measurement done on a mitral-granule cell mass (Freeman 1975, 1979a; Fig. 3). Both the mitral and granule cells have a membrane time

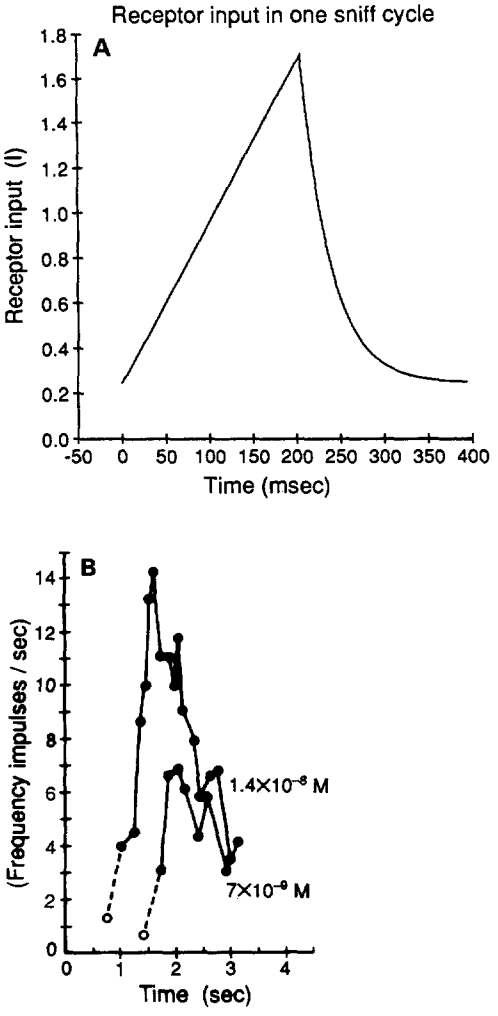

Fig. 4. A Model of receptor cell response time course to odors in a sniff cycle. **B** Experimentally measured receptor firing frequency with an odor pulse delivered to the nose, two concentration examples of odor plotted, the line below the time axis indicates the odor pulse duration. Taken from Getchell and Shepherd (1978)

constant of 5–10 ms (Freeman and Skarda 1985; Shepherd, Private Communication). Very little is known about the functional strength of synapses in the olfactory bulb.

The receptor cell firing rate increases from the spontaneous background level of 1–3 impulses/s with increasing odor concentration (Getchell and Shepherd 1978), and may reach 10–60 impulses/s. With odor pulses delivered to the mucosa, the receptor firing rate increases approximately linearly in time as long as the pulse is not too long, and then terminates quickly, sometimes as fast as 100 ms, after the odor pulse terminates (Fig. 4). High resolution 2-deoxyglucose autoradiography experiment (Lancet et al. 1982) shows that for an input odor, different and even neighboring glomeruli have different activity levels, while the activity is relatively uniform within a single glomerulus. Little is known about the input from the higher centers to the bulb.

Stimulation with odors, depending on the animal motivation, causes an onset of a high-amplitude bulbar oscillatory activity, which is detected by surface EEG electrodes and returns to a low-amplitude oscillation on the cessation of odor stimulus (Freeman 1978). The oscillation is an intrinsic property of the bulb itself persisting after the central connections to the bulb is cut off (Freeman and Skarda 1985). Central inputs (Freeman 1979a; Freeman and Skarda 1985; Baird 1986) influence oscillation onset; the oscillation exists only in motivated animals, and can be present without an input odor (Freeman 1978). However, the oscillation disappears when the nasal air flow is blocked (Freeman and Schneider 1982). The granule cells are the generators of the surface EEG wave, for the mitral cells produce a closed monopole field which is negligible at bulbar surface (Freeman 1975). The EEG (Freeman 1978; Freeman and Schneider 1982) shows a high amplitude oscillation arising during the inhalation and stopping early in the exhalation. The oscillation bursts have a peak frequency in the range of 35–90 Hz, and ride on a slow background wave phase locked with the respiratory wave. Different parts of the bulb have the same dominant frequency but different amplitudes and phases. A specific odor input will set a specific EEG oscillation pattern across the olfactory bulb.

3 Model Organization

For comparisons between experiments and theory of the olfactory bulb, it is essential to model with realism. To do the mathematical analysis and simulation necessary to understand collective and statistical properties, it is necessary to disregard superfluous details. Our model organization is a compromise between these two considerations.

3.1 General Model Structure

Only the mitral and granule cells are included in the bulb model. The glomerular layer structure is neglected, and the receptor input is regarded as effectively directed onto the mitral cells. The tufted cells are considered as mitral cells, and the interneural short axon cells are neglected because they are very few in number compared with the granule cells. Both the receptor and central inputs are included. There are N (excitatory) mitral cells and M (inhibitory) granule cells in the model. Although the mathematical analysis puts no limit on the absolute cell numbers, the following cell

number reductions are used in the computer simulation because of the limited computer capability. The group of mitral cells connecting to the same glomerulus is simplified into one cell by assuming that the activity level changes little locally. Similarly, the ratio $M:N$ is taken to be much less than the 200:1 in the real bulb. Excitation and inhibition are kept in balance by correspondingly increasing the strength of the granule cell (inhibitory) synapses.

3.2 Inputs to the Bulb Model

The inputs from outside bulb to a mitral cell i is described by the components I_i for $1 \leqq i \leqq N$. This input vector I is a superposition of a true odor signal and a background input, i.e., $I = I_{\text{odor}} + I_{\text{background}}$. $I_{\text{background}}$ is the sum of the receptor background input and the central inputs to the mitral cell dendrites in the input layer. I_{odor} ranges from zero to 10 or 20 times of $I_{\text{background}}$, determined by odor pattern P_{odor}, with components $P_{\text{odor},i}$ for $1 \leqq i \leqq N$, characterizing the odor concentration and the receptor cells' sensitivity pattern to the odor. Each sniff cycle lasts for 200–500 ms as that of a rabbit. All these inputs are taken to be excitatory. The odor concentration on the mucosa will rise rapidly at the initiation of inhale, and correspondingly drop at initial exhale because of absorption by the lungs. Odorant diffusion through the mucous to the receptors should delay the increase in receptor activities. Thus we model the I_{odor} to increase in time during inhale, as observed in experiment (Getchell and Shepherd 1978). Exhalation is modeled as an exponential return toward the ambient. Then for any mitral cell i exposed to odor,

$$I_{\text{odor},i}(t) = \begin{cases} P_{\text{odor},i} \cdot (t - t^{\text{inhale}}) + I_{\text{odor},i}(t^{\text{inhale}}), \\ \quad \text{if} \quad t^{\text{inhale}} \leqq t \leqq t^{\text{exhale}}; \\ I_{\text{odor},i}(t^{\text{exhale}}) \cdot e^{-(t - t^{\text{exhale}})/\tau_{\text{exhale}}}, \\ \quad \text{if} \quad t > t^{\text{exhale}}, \end{cases} \tag{3.1}$$

as illustrated in Fig. 4, where $\tau_{\text{exhale}} = 33$ ms and t^{inhale} and t^{enhale} are the on-set times for inhale and exhale respectively.

The central input to the granule cells are described by the vector I_c with components $I_{c,j}$ for $1 \leqq j \leqq M$. For now, it is assumed that I_c and $I_{\text{background}}$ do not change during a sniff cycle. The scales of $I_{\text{background}} = 0.243$ and $I_c = 0.1$ are set such that when $I_{\text{odor}} = 0$, most of the mitral and granule cells have their cell internal state just below maximum slope points on their input-output function curves (Freeman 1979a). So there will be weak incoherent oscillatory activity when there is no odor input, as often observed (Freeman and Schneider 1982).

3.3 The Model Cell Property

Each cell is modeled as one unit since typical (dendrodendritic) interactions take place locally on the dendrites with electrotonic length less than one (Shepherd 1979). The internal state level of a neuron is described by a single variable resembling the cell membrane potential. Those of the mitral cells and granule cells are respectively $X = \{x_1, x_2, \ldots, x_N\}$ and $Y = \{y_1, y_2, \ldots, y_M\}$. The cell output is described as a continuous function of the cell's internal state, and can be thought of as proportional to the cell firing frequency. They are $G_x(X) = \{g_x(x_1), g_x(x_2), \ldots, g_x(x_N)\}$ and $G_y(Y) = \{g_y(y_1), g_y(y_2), \ldots, g_y(y_M)\}$ for the mitral and granule cells respectively, where g_x and g_y are the neurons' output functions which have the following properties modeled after a real cell:

1) $g_x(g_y) \geqq 0$, $g'_x(g'_y) \geqq 0$, i.e., the output firing rate is non-negative and non-decreasing with increasing cell membrane potential.

2) g_x and g_y are non-linear, the strongest non-linear region occurs around the firing threshold region of the cell, and the outputs also saturate at high internal state level.

Figure 3 shows the form of input-output relation used for mitral and granule cells. The complicated mathematical form was chosen for convenience, and is inessential to the behavior as long as the shapes are qualitatively preserved.

The function formulae are:

$$g_x(x) = \begin{cases} S'_x + S'_x \cdot \tanh\left(\dfrac{x - th}{S'_x}\right), & \text{if} \quad x < th; \quad S'_x = 0.14, \\ S'_x + S_x \cdot \tanh\left(\dfrac{x - th}{S_x}\right), & \text{if} \quad x \geqq th. \quad S_x = 1.4. \end{cases}$$

$$g_y(y) = \begin{cases} S'_y + S'_y \cdot \tanh\left(\dfrac{y - th}{S'_y}\right), & \text{if} \quad y < th; \quad S'_y = 0.29, \\ S'_y + S_y \cdot \tanh\left(\dfrac{y - th}{S_y}\right), & \text{if} \quad y \geqq th; \quad S_y = 2.9, \end{cases}$$

where $th = 1$. The granule cells were modeled with a larger linear range, reflecting the fact that granule cells do not have axons, and thus have a less strong non-linear threshold effect. The non-linear and threshold functions are essential for the bulbar oscillation dynamics (Freeman 1979a; Freeman and Skarda 1985; Baird 1986) to be studied.

3.4 The Synaptic Connections and System Dynamics

The geometry of bulbar structure, namely with cells sitting on two dimensional sheets shaped like a seg-

ment of a sphere, is simplified as cells sitting on a one dimensional ring. Each cell is specified by an index, e.g. i^{th} mitral cell, and j^{th} granule cell for all i, j which resemble the spatial location of the cells. The i^{th} mitral cell is the neighbor of $i \pm 1^{th}$ mitral cells and $\frac{i \cdot M^{th}}{N}$ granule cell. The 1^{st} and the N^{th} (M^{th}) mitral (granule) cells are next to each other. This 1 – d simplification is helpful for understanding but is not essential for the model (see discussion).

The synaptic strength in the model is postsynaptic input: presynaptic output. An $N \times M$ matrix H_0 and $M \times N$ matrix W_0 are used respectively to describe the synaptic connection from granule cells to mitral cells and vice versa. For instance, $H_{0,ij}$ is the connection strength from the j^{th} granule cell to i^{th} mitral cell. Since the synaptic connection in the bulb is local, $H_{0,ij} \neq 0$ only if j^{th} granule cell and i^{th} mitral cell are near each other, i.e., $j \approx \frac{i \cdot M}{N}$ or $j \approx \frac{i \cdot M}{N} + M$ because of the ring structure. This implies that H_0 will be a near diagonal matrix with most non-zero elements near the diagonal line. Here diagonal elements mean those $H_{0,ij}$ with $j = \frac{i \cdot M}{N}$, because H_0 need not be a square matrix. W_0 has a similar matrix structure. The matrices used in the computer simulations are (for $N = M = 10$):

$$H_0 = \begin{pmatrix} 0.3 & 0.9 & 0 & 0 & 0 & 0 & 0 & 0 & 0 & 0.7 \\ 0.9 & 0.4 & 1.0 & 0 & 0 & 0 & 0 & 0 & 0 & 0 \\ 0 & 0.8 & 0.3 & 0.8 & 0 & 0 & 0 & 0 & 0 & 0 \\ 0 & 0 & 0.7 & 0.5 & 0.9 & 0 & 0 & 0 & 0 & 0 \\ 0 & 0 & 0 & 0.8 & 0.3 & 0.8 & 0 & 0 & 0 & 0 \\ 0 & 0 & 0 & 0 & 0.7 & 0.3 & 0.9 & 0 & 0 & 0 \\ 0 & 0 & 0 & 0 & 0 & 0.7 & 0.4 & 0.9 & 0 & 0 \\ 0 & 0 & 0 & 0 & 0 & 0 & 0.5 & 0.5 & 0.7 & 0 \\ 0 & 0 & 0 & 0 & 0 & 0 & 0 & 0.9 & 0.3 & 0.9 \\ 0.9 & 0 & 0 & 0 & 0 & 0 & 0 & 0 & 0.8 & 0.3 \end{pmatrix},$$

$$W_0 = \begin{pmatrix} 0.3 & 0.7 & 0 & 0 & 0 & 0 & 0 & 0 & 0.5 & 0.3 \\ 0.3 & 0.2 & 0.5 & 0 & 0 & 0 & 0 & 0 & 0 & 0.7 \\ 0 & 0.1 & 0.3 & 0.5 & 0 & 0 & 0 & 0 & 0 & 0 \\ 0 & 0.5 & 0.2 & 0.2 & 0.5 & 0 & 0 & 0 & 0 & 0 \\ 0.5 & 0 & 0 & 0.5 & 0.1 & 0.9 & 0 & 0 & 0 & 0 \\ 0 & 0 & 0 & 0 & 0.3 & 0.3 & 0.5 & 0.4 & 0 & 0 \\ 0 & 0 & 0 & 0.6 & 0 & 0.2 & 0.3 & 0.5 & 0 & 0 \\ 0 & 0 & 0 & 0 & 0 & 0 & 0.5 & 0.3 & 0.5 & 0 \\ 0 & 0 & 0 & 0 & 0 & 0.2 & 0 & 0.2 & 0.3 & 0.7 \\ 0.7 & 0 & 0 & 0 & 0 & 0 & 0 & 0.2 & 0.3 & 0.5 \end{pmatrix}. \quad (3.2)$$

Most of the non-zero elements are near the diagonal line and corners, reflecting the assumed ring geometry. Non-zero elements in W_0 occur further from the diagonal line than those in H_0, reflecting the longer range mitral-to-granule than granule-to-mitral connections.

The bulb model system has equation of motion:

$$\begin{aligned} \dot{X} &= -H_0 G_y(Y) - \alpha_x X + I, \\ \dot{Y} &= W_0 G_x(X) - \alpha_y Y + I_c, \end{aligned} \quad (3.3)$$

where $\alpha_x = 1/\tau_x$, $\alpha_y = 1/\tau_y$, and $\tau_x = \tau_y = 7$ ms are the time constants of the mitral and granule cells respectively. The minus sign in front of the matrix H_0 represents the inhibitory nature of the granule cells. In simulation, weak random noise with a 9 ms correlation time is added to I and I_c to simulate the fluctuations in the system.

The scales of H_0 and W_0 are chosen to be about the same, with values such that the oscillation frequency in the stimulated model bulb neural activity is about the same as in the real biological bulb (see Sect. 5.1). The individual elements of H_0 and W_0 in simulation are chosen such that there will be high amplitude oscillations in the model bulb for certain kinds of odor input I_{odor} (see Sect. 6.1).

4 Simulation Result

Computer simulation was done with 10 mitral and granule cells. The simulations start with initial cell internal states close to the background state when no odor inputs are present. Different odor input patterns are represented by the different vectors P_{odor}.

Figure 5 shows the simulation result of several sniff cycles of a certain odor input I_{odor}. The rise and fall of oscillations with input and the baseline shift wave phase locked with sniff cycles are obvious. The surface EEG wave is calculated using the approximation by Freeman (1980) as a weighted sum of each granule cell output $g_y(y_j)$. Physiologically measured EEG waves are shown for comparison.

The activities of individual cells in a sniff cycle across the whole bulb constitute an activity pattern for the particular odor input I_{odor} (Fig. 6). All the cells oscillate coherently with the same frequency as physiologically observed (Freeman 1978; Freeman and Schneider 1982). The mitral cell output pattern is the only output of the bulb. Physiological multi-channel measurement of surface EEG waves (Freeman 1978), though originating in the granule cell activities, also displays a similar information pattern in multi-dimensions. For comparison, both the simulated and measured (band-pass filtered) EEG patterns are included in the figure.

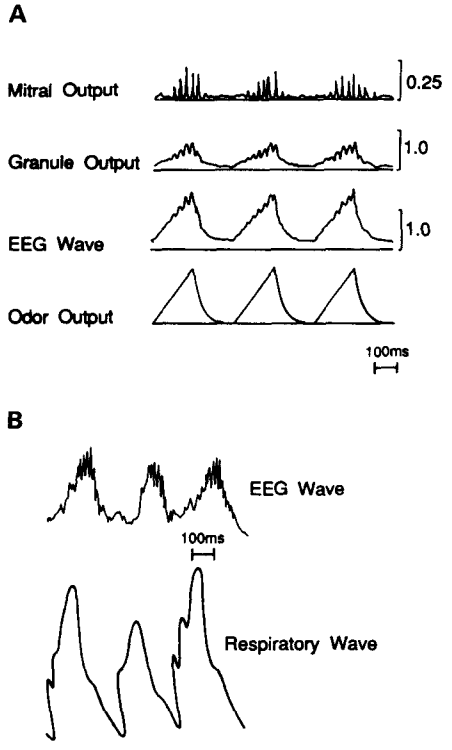

Fig. 5. A Simulation result of bulbar response in several sniff cycles. **B** Experimentally measured EEG waves with odor inputs, taken from Freeman and Schneider (1982). Both the simulated and measured EEG waves are surface negative waves

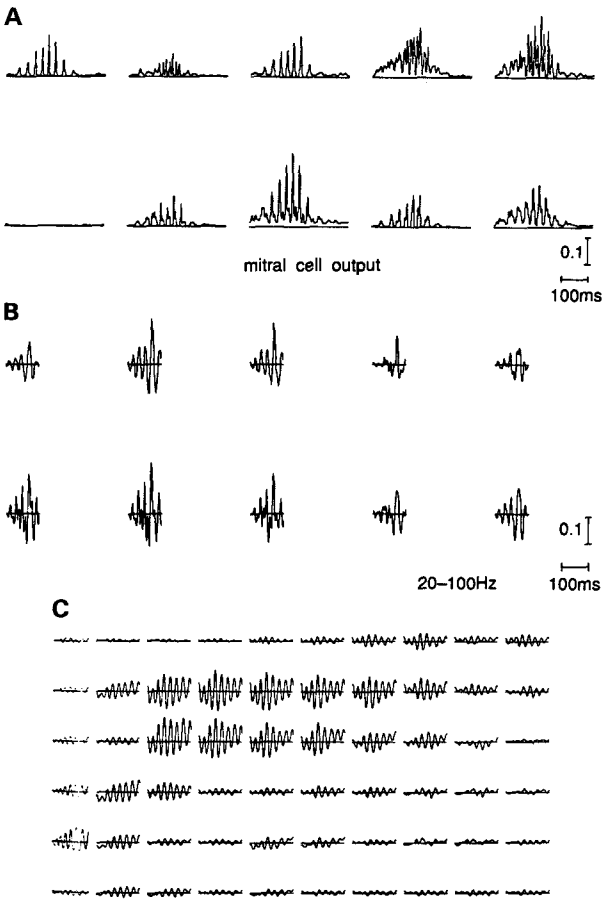

Fig. 6. A Simulated mitral cell output pattern in one sniff cycle with one odor input example. **B** Segment of a simulated surface EEG wave pattern during the oscillatory bursts with the same odor input as in **A**. **C** Multi-channel recorded bulbar surface EEG wave pattern during 100 ms of bursts, taken from Freeman (1978). Both signals in **B** and **C** are band-pass filtered

These simulation results show that the model bulb can capture the major known effects of the real bulb. Furthermore, the model shows the capability of a pattern classifier. For a sniff cycle lasting $t_s = 370$ ms in simulation with fixed inhale and exhale time, some input patterns P_{odor} induce oscillation, while others do not, and different P_{odor} induce different oscillation patterns (Fig. 7). Zero odor input $P_{\text{odor}} = 0$ induces little activity above background, which is the case observed when the nasal airflow is blocked (Freeman and Schneider 1982). What patterns drive the bulb well is as yet arbitrary in our model, for there is no relation between the particular connections and the odors which are used.

Some measures have been defined to describe the difference between different patterns. The mitral output $G_x(X(t))$ were band-pass filtered above 20 Hz to obtain the oscillatory signal $S_h(t)$, and low-pass below 20 Hz for baseline shift $S_l(t)$. The oscillation period T is the time lag $\geqq 5$ ms which gives the largest autocorrelation for $S_h(t)$. Similarly, oscillation phase differences of the different mitral cells are calculated by cross-correlating the different components of $S_h(t)$ after the higher frequency components ($f > 1.3/T$) are removed. The phase differences are measured with respect to the first cell. The oscillation amplitude of i^{th} cell is the root-mean-square of $S_{h,i}(t)$ averaged in time. The results show that for each response, cells with substantial oscillation amplitudes have frequencies within 1 Hz of each other. Define

O_{osci}: an N-dimensional complex vector describing the dominant frequency oscillation amplitudes and phases averaged over the sniff cycle;

O_{mean}: an N-dimensional real vector describing the baseline activities above the background level ($S_l(t) - S_l(t)|_{P_{\text{odor}}=0}$) averaged over the sniff cycle;

$\bar{O}_{\text{mean}}$ and $\bar{O}_{\text{osci}}$: scalars describing the root-mean-square average of the components of O_{mean} and O_{osci} respectively.

We can use these quantities to define the similarity or difference between response patterns. For two

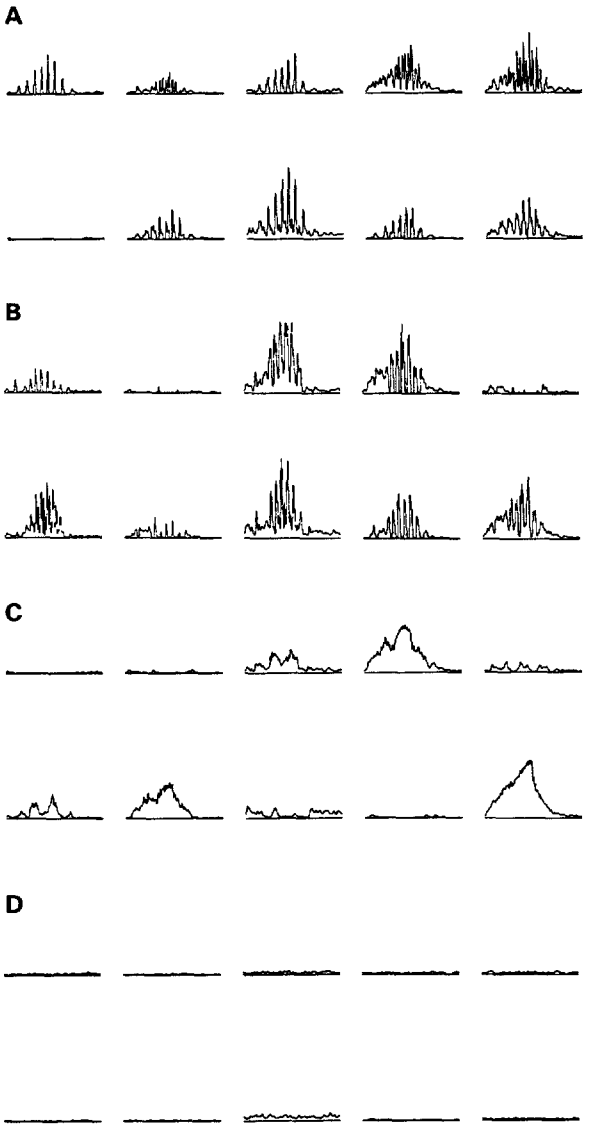

Fig. 7A–D. Mitral output response patterns for different inputs I_{odor} of one sniff cycle lasting 370 ms. **A, B** Oscillatory responses for two different inputs. **C** Non-oscillatory response for an input. **D** Response for no odor inputs

response patterns a and b denoted by superindices, possible distance measures are:

$$d_1 = 1 - \frac{\langle O^a_{\text{mean}} O^b_{\text{mean}} \rangle}{|O^a_{\text{mean}}|\,|O^b_{\text{mean}}|},$$

$$d_2 = 1 - \frac{|\langle O^a_{\text{osci}} O^b_{\text{osci}} \rangle|}{|O^a_{\text{osci}}|\,|O^b_{\text{osci}}|},$$

$$d_3 = \frac{\bar{O}^a_{\text{mean}} - \bar{O}^b_{\text{mean}}}{\bar{O}^a_{\text{mean}} + \bar{O}^b_{\text{mean}}},$$

$$d_4 = \frac{\bar{O}^a_{\text{osci}} - \bar{O}^b_{\text{osci}}}{\bar{O}^a_{\text{osci}} + \bar{O}^b_{\text{osci}}}, \tag{4.1}$$

Table 1. Differences between two patterns. Data in each group is the average of three pairs of patterns. Group one: The two patterns in each pair have different odor inputs. Group two: The two patterns in each pair have the same odor input but different system fluctuations

	d_1	d_2	$\lvert d_3\rvert$	$\lvert d_4\rvert$	d_1^{in}	$\lvert d_3^{\text{in}}\rvert$
Group one	0.3217	0.4243	0.1403	0.2840	0.0257	0.1657
Group two	0.0007	0.0560	0.0050	0.0413	0	0

where $\langle\ \rangle$ and $|\ |$ denote the dot product and absolute value respectively. d_1 and d_2 give differences in the response pattern forms, while d_3 and d_4 give differences in the response amplitudes.

For comparison, d_1^{in}, which is indicative of the difference in form (not amplitude) of the input patterns P_{odor}, is calculated by replacing O_{mean} with P_{odor} in (4.1) for d_1 (similar calculation is done for d_3^{in} corresponding to d_3). Table 1 shows that the bulb amplifies the differences in input vector P_{odor} to give output vectors O_{osci} and O_{mean} (compare d_1^{in} with d_1 and d_2), while the responses to same odor with different noise samples differ negligibly. The noise amplitudes are not crucial for the structure of the oscillation patterns.

5 Mathematical Analysis

5.1 Olfactory Bulb as a Group of Coupled Non-Linear Oscillators

An oscillator with frequency ω can be described by the differential equations

$$\begin{aligned} \dot{x} &= -\omega y \\ \dot{y} &= \omega x \end{aligned} \quad \text{or} \quad \ddot{x} + \omega^2 x = 0 \tag{5.1}$$

with solution:

$$x = r_0 \sin(\omega t + \phi) \qquad y = -r_0 \cos(\omega t + \phi),$$

where r_0 and ϕ are arbitrary real constants. The $x(t)$, $y(t)$ trajectory is a circle. With dissipation, (5.1) becomes

$$\begin{aligned} \dot{x} &= -\omega y - \alpha x \\ \dot{y} &= \omega x - \alpha y \end{aligned} \quad \text{or} \quad \ddot{x} + 2\alpha\dot{x} + (\omega^2 + \alpha^2)x = 0. \tag{5.2}$$

The solution becomes

$$x = r_0 e^{-\alpha t} \sin(\omega t + \phi),$$

where α is the dissipation constant. If a mitral cell and a granule cell are connected to each other, with inputs $i(t)$ and $i_c(t)$ respectively, then

$$\begin{aligned} \dot{x} &= -h \cdot g_y(y) - \alpha_x x + i(t), \\ \dot{y} &= w \cdot g_x(x) - \alpha_y y + i_c(t). \end{aligned} \tag{5.3}$$

This is the scalar version of (3.3) with each upper case letter representing a vector or matrix replaced by a lower case letter representing a scalar. It is assumed that $i(t)$ has a much slower time course than x or y, because the frequency of sniffs is considerably lower than the characteristic neural oscillation frequency, and that i_c, input from higher centers, will be kept fixed. We can then use the adiabatic approximation, and define the equilibrium point (x_0, y_0) as

$$\begin{aligned} \dot{x}_0 \approx 0 &= -h \cdot g_y(y_0) - \alpha_x x_0 + i, \\ \dot{y} \approx 0 &= w \cdot g_x(x_0) - \alpha_y y_0 + i_c. \end{aligned} \tag{5.4}$$

Define $x' \equiv x - x_0$, $y' \equiv y - y_0$. Then

$$\begin{aligned} \dot{x}' &= -h(g_y(y) - g_y(y_0)) - \alpha_x x', \\ \dot{y}' &= w(g_x(x) - g_x(x_0)) - \alpha_y y'. \end{aligned}$$

This is already similar to (5.2). If we omitted the dissipation, $\alpha_x = \alpha_y = 0$, then, when x' and y' are small, they oscillate along the solution orbit

$$R \equiv \int_{x_0}^{x_0 + x'} w(g_x(s) - g_x(x_0))\mathrm{d}s + \int_{y_0}^{y_0 + y'} h(g_y(s) - g_y(y_0))\mathrm{d}s = \text{constant}$$

which is a closed curve in the original (x, y) space surrounding the point (x_0, y_0). This means (x, y) will oscillate around the point (x_0, y_0). The oscillation becomes strictly sinusoidal if g's are linear functions. When the dissipation is included, the orbit in (x, y) space will spiral into the point (x_0, y_0):

$$\begin{aligned} \mathrm{d}R/\mathrm{d}t = &-\alpha_x w(g_x(x) - g_x(x_0))(x - x_0) \\ &-\alpha_y h(g_y(y) - g_y(y_0))(y - y_0). \end{aligned}$$

Therefore, a connected pair of mitral and granule cells behaves as a damped non-linear oscillator, whose oscillation center (x_0, y_0) is determined by the external inputs i and i_c. If the oscillation amplitude is small, then the system can be approximated by a damped sinusoidal oscillator via linearization around the point (x_0, y_0):

$$\begin{aligned} \dot{x} &= -h \cdot g_y'(y_0) y - \alpha_x x, \\ \dot{y} &= w \cdot g_x'(x_0) x - \alpha_y y, \end{aligned} \tag{5.5}$$

where (x, y) are now the deviation from (x_0, y_0). The solution is

$$x = r_0 \mathrm{e}^{-\alpha t} \sin(\omega t + \phi),$$

where $\alpha = (\alpha_x + \alpha_y)/2$ and $\omega = \sqrt{hwg_x'(x_0)g_y'(y_0) + (\alpha_x - \alpha_y)^2/4}$. If $\alpha_x = \alpha_y$, which is about right in the bulb, then $\alpha = \alpha_x = \alpha_y$, $\omega = \sqrt{hwg_x'(x_0)g_y'(y_0)}$. Using the bulbar cell time constant and the oscillation frequency from the previous section, $\alpha \approx 0.3\omega$. The scale of synaptic connections strength was chosen so that the model bulb oscillation frequency agrees with the biological data (Sect. 3.4). The effect of the input controlled equilibrium point (x_0, y_0) on the frequency implies that the oscillation frequency is modulated by the receptor and central input in the real system. The equilibrium point (x_0, y_0) is always stable, i.e., the non-linear oscillation is always damped, and no sustained oscillation will exist unless driven by an external oscillating input.

N such mitral-granule pairs without interconnections between the pairs, represent a group of N independent damped non-linear oscillators. If the cells in one oscillator also connect to cells in the neighboring oscillators, then these oscillators are no longer independent. This is exactly the situation in the olfactory bulb. A granule cell receiving inputs from a certain mitral cell gives outputs to other mitral cells as well. Similarly, a mitral cell has outputs also to granule cells which do not give outputs to this mitral cell. The locality of synaptic connections in the bulb implies that the oscillator coupling is also local. (That there are many more granule cells than mitral cells only means that there is more than one granule cell in each oscillator.) This situation can be quantitatively treated by including many neurons in the mathematical analysis.

Proceeding as in the single oscillator case,

$$\begin{aligned} \dot{X} &= -H_0 G_y(Y) - \alpha_x X + I(t), \\ \dot{Y} &= W_0 G_x(X) - \alpha_y Y + I_c(t), \end{aligned} \tag{5.6}$$

[cf. (5.3)]. Use the adiabatic approximation and define the equilibrium point (X_0, Y_0) as

$$\begin{aligned} \dot{X}_0 \approx 0 &= -H_0 G_y(Y_0) - \alpha_x X_0 + I, \\ \dot{Y}_0 \approx 0 &= W_0 G_x(X_0) - \alpha_y Y_0 + I_c, \end{aligned} \tag{5.7}$$

linearize around (X_0, Y_0),

$$\begin{aligned} \dot{X} &= -H_0 G_y'(Y_0) Y - \alpha_x X, \\ \dot{Y} &= W_0 G_x'(X_0) X - \alpha_y Y, \end{aligned} \tag{5.8}$$

where (X, Y) are now deviations from (X_0, Y_0) and $G_x'(X_0)$ and $G_y'(Y_0)$ are diagonal matrices with elements: $[G_x'(X_0)]_{ii} = g_x'(x_{i,0})$, $[G_y'(Y_0)]_{jj} = g_y'(y_{j,0})$, for all i, j. Define $H \equiv H_0 G_y'(Y_0)$, $W \equiv W_0 G_x'(X_0)$, so

$$\begin{aligned} \dot{X} &= -HY - \alpha_x X, \\ \dot{Y} &= WX - \alpha_y Y. \end{aligned} \tag{5.9}$$

Eliminating Y,

$$\ddot{X} + (\alpha_x + \alpha_y)\dot{X} + (A + \alpha_x \alpha_y)X = 0, \tag{5.10}$$

where $A \equiv HW = H_0 G_y'(Y_0) W_0 G_x'(X_0)$. This is the equation for the system of N coupled oscillators [cf. (5.2)]. The second term $(\alpha_x + \alpha_y)\dot{X}$ describes the dissipation, while the third term $(A + \alpha_x \alpha_y)X$ includes also

the indirect couplings between different mitral cells via the granule cells. The i^{th} oscillator (mitral cell) follows the equation

$$\ddot{x}_i+(\alpha_x+\alpha_y)\dot{x}_i+(A_{ii}+\alpha_x\alpha_y)x_i+\sum_{j\neq i}A_{ij}x_j=0. \quad (5.11)$$

The first three terms are like a single (i^{th}) oscillator [cf. (5.2)], while the last term describes the coupling to other oscillators. These oscillator couplings are local because the matrix A is near diagonal, which follows from the definition of A and the fact that both H_0 and W_0 are near diagonal. The elements of matrix A are non-negative by the definition. The coupling from j^{th} oscillator to i^{th} oscillator goes through the connection path from j^{th} mitral cell to i^{th} mitral cell via all those intermediate granule cells. In particular, A_{ii} originates from the connection path from i^{th} mitral cell back to itself via the intermediate granule cells. In our simulated example, the H_0 and W_0 used implies that each cell connects to about three neighboring cells, so from above argument each oscillator couples to about 5 neighboring oscillators.

The set of mitral and granule cells in the blub can thus be viewed as a group of locally coupled non-linear damped oscillators. The system can be approximated by linear oscillators if the oscillation amplitude is small enough. Non-linear effect will occur when the amplitude is large, and the oscillation wave form will then become non-sinusoidal.

This model of the olfactory bulb can be generalized to other masses of interacting excitatory and inhibitory cells such as those in olfactory cortex, neocortex and hippocampus (Shepherd 1979) etc. where there may as well be connections between the excitatory cells and between the inhibitory cells, as is claimed by some for the olfactory bulb (Nicoll 1971; Freeman 1975, 1979b, c). Suppose that B_0 and C_0 are excitatory-to-excitatory and inhibitory-to-inhibitory connection matrices respectively, then (5.6) becomes:

$$\begin{aligned}\dot{X}&=-H_0G_y(Y)-\alpha_xX+B_0G_x(X)+I(t),\\ \dot{Y}&=W_0G_x(X)-\alpha_yY-C_0G_y(Y)+I_c(t).\end{aligned} \quad (5.12)$$

Consequently (5.10) becomes

$$\ddot{X}+(\alpha_x-B+\alpha_y+C)\dot{X}+(A+(\alpha_x-B)(\alpha_y+C))X=0, \quad (5.13)$$

where $B\equiv B_0G_x'(X_0)$ and $C\equiv HC_0G_y'(Y_0)H^{-1}$ (H^{-1} is the pseudo-inverse of H). If we replace α_x by α_x-B, and α_y by α_y+C, then (5.10) becomes (5.13). This means that if coupling B and C is local (i.e., almost diagonal), having excitatory connections B_0 is like reducing dissipation for oscillators, while having the inhibitory connections is like adding some oscillator dissipation. Strong enough local excitatory-to-excitatory connections B_0 can reduce the oscillator dissipations so much that the net can oscillate even without much odor input I_{odor} as is simulated by Freeman (1979b, c). This is however not necessarily true if the connections B_0 are non-local (as in the olfactory cortex, Haberly 1985), since a negative dissipation introduced by a local excitatory-to-excitatory connection can become positive non-locally when the two oscillators coupled by B are oscillating with opposite phases.

5.2 *Oscillation Pattern Analysis*

If X_k is one of the eigenvectors of A with eigenvalue λ_k, (5.10) has N independent modes

$$\begin{aligned}X&\propto X_k e^{i\omega_k t}\\ &\equiv X_k\exp\left(-\frac{(\alpha_x+\alpha_y)}{2}t\pm i\sqrt{\lambda_k+\frac{(\alpha_x-\alpha_y)^2}{4}}\,t\right)\end{aligned} \quad (5.15)$$

for $k=1,2,\ldots,N$, where ω_k is the complex frequency of the oscillation mode. We will denote X_k as the k^{th} oscillation mode of the system. For simplicity, we set $\alpha_x=\alpha_y=\alpha$, then

$$X\propto X_k e^{-\alpha t\pm i\sqrt{\lambda_k}t} \quad (5.16)$$

for all k. Each mode has frequency $\mathrm{Re}\sqrt{\lambda_k}$, where Re means the real part of a complex number. The relative phases and amplitudes of the individual oscillators in k^{th} mode are described by the individual components of complex vector X_k. If $\mathrm{Re}(-\alpha\pm i\sqrt{\lambda_k})>0$ is satisfied for some k, then the amplitude of the k^{th} mode will increase with time, i.e., it is a growing oscillation.

Starting from an initial condition of arbitrary small amplitudes in linear analysis, the mode with the fastest growing amplitude will dominate the output. When there is a single dominating mode, the whole bulb will oscillate in the same frequency as observed physiologically (Freeman 1978; Freeman and Schneider 1982) as well as in the simulation. When the non-linear effect is considered, the strongest modes will suppress the others, and the final activity output will be a single "mode" in a non-linear regime.

The collective oscillation mode is a result of coupling. Each oscillator gets external driving "forces" from the neighboring oscillators. When they influence each other in harmony, a global oscillation mode results. The amplitude of an oscillator will increase when its driving "force" is larger than its damping "force". An oscillation mode with growing amplitude emerges when each oscillator with substantial amplitude in the mode has enough driving "force" through coupling with other oscillators. Recall that a single oscillator in our analysis is always damped, which means that the equilibrium point (x_0, y_0) is always stable. Because of coupling between the oscillators, the

equilibrium point (X_0, Y_0) of a *group* of oscillators *is no longer always stable* with the possibility of growing oscillation modes.

In order that some mode X_k can be both a growing and oscillatory mode, λ_k must be complex. For this, a necessary (but not sufficient) condition is that matrix A is non-Hermitian. It follows that systems of less than three oscillators will not have growing modes, since if A is real and is of dimension 1 or 2, it will only have real eigenvalues.

For illustration, for the symmetric matrix

$$A=\begin{pmatrix} a & b & 0 & 0 & & \dots & & 0 & b \\ b & a & b & 0 & & \dots & & 0 & 0 \\ 0 & b & a & b & 0 & 0 & \dots & 0 & 0 \\ \vdots & \vdots & & & & \dots & \ddots & & \vdots \\ b & 0 & & & \dots & & 0 & b & a \end{pmatrix}. \tag{5.17}$$

The N oscillation modes will be

$$\begin{pmatrix} \sin(k1) \\ \sin(k2) \\ \vdots \\ \sin(ki) \\ \vdots \\ \sin(kN) \end{pmatrix} e^{-\alpha t \pm i\sqrt{\lambda_k}t} \quad \begin{pmatrix} \cos(k1) \\ \cos(k2) \\ \vdots \\ \cos(ki) \\ \vdots \\ \cos(kN) \end{pmatrix} e^{-\alpha t \pm i\sqrt{\lambda_k}t}, \tag{5.18}$$

where $k=\frac{2\pi K}{N}$, K is an integer, $0 \leqq K < \frac{N}{2}$, $\lambda_k = a + 2b\cos(k)$. For $b<a/2$, $\lambda_k>0$, all the modes will be damped oscillations with similar frequencies close to $\omega=\sqrt{a}$. Notice that in each mode, all the oscillators have the same oscillation phase, but with different amplitudes. If we have a non-symmetric matrix

$$A=\begin{pmatrix} a & b & c & 0 & & \dots & & 0 & 0 \\ 0 & a & b & c & & \dots & & 0 & 0 \\ 0 & 0 & a & b & c & 0 & \dots & 0 & 0 \\ \vdots & \vdots & & & & \dots & \ddots & & \vdots \\ c & 0 & & & \dots & & 0 & a & b \\ b & c & & & \dots & & 0 & 0 & a \end{pmatrix} \tag{5.19}$$

then the oscillation modes will be

$$\begin{pmatrix} e^{i\beta} \\ e^{2i\beta} \\ \vdots \\ e^{im\beta} \\ \vdots \\ e^{iN\beta} \end{pmatrix} e^{-\alpha t \pm i\sqrt{\lambda_\beta}t} \qquad \begin{aligned} &\beta = 2\pi K/N, \\ &K \text{ is an integer}, \\ &0 \leqq K < N, \\ &\lambda_\beta = a + b e^{i\beta} + c e^{2i\beta}. \end{aligned} \tag{5.20}$$

Notice that in this case λ_β's are non-real complex numbers. It is possible to have growing modes if for some β, $\mathrm{Re}(-\alpha \pm i\sqrt{\lambda_\beta})>0$. Also notice that the individual oscillators in most modes have different oscillation phases.

5.3 Explanation of Olfactory Bulb Activities

One prediction of this model is that the local mitral cells' oscillation phase leads that of the local granule cells by a quarter cycle, as is clear already from the single oscillator analysis. This is confirmed in experiments (Freeman 1975) in which the local mitral cell unit activity was compared with the granule cell generated surface EEG waves for phase difference. [Note that the orientation of the granule cell dipole field gives the surface EEG wave an opposite sign to that of granule cell activities (Freeman 1975). Therefore the sign of the EEG oscillation is to be reversed before comparing it with the local mitral cell oscillation for phase difference.]

A second property of the model is that for any particular stimulus, oscillatory activity should have the same dominant frequency everywhere on the bulb. This is also true in experiments (Freeman 1978; Freeman and Schneider 1982). Furthermore, the range of oscillation frequencies possible should be narrow. The observed range covers 35–90 Hz. A damped oscillator will not have high amplitude response unless the frequency of the external driving force is close to the oscillator resonant frequency. Therefore, an oscillation mode will not be non-damping unless its frequency, which is the frequency of the driving force for the oscillators in the system, is close to the oscillator resonant frequencies.

A third feature of the model is the non-zero phase gradient field across the bulb, as suggested by the examples in Sect. (5.2), which is also present in the physiologically observable oscillations. In order that the i^{th} damping oscillator with frequency ω sustains its oscillation amplitude, the external driving force $F_i \equiv -A_{ij}x_j$ should be relatively in phase with the velocity $\dot{x}_i$ of the oscillator, so that the "energy" inflow from external force is no less than the dissipation. If all the coupling oscillators x_j are in phase with x_i, such "energy" transfer can not occur since F_i is perpendicular to $\dot{x}_i$. An excited oscillator in a growing mode requires coupling to neighbors oscillating with phases different from its own. Only those oscillations with non-zero phase gradient field can be stable or grow. This will not be necessarily true if the excitatory-to-excitatory connections or other synaptic connection types are present, since the nature of oscillator coupling will be different [see (5.13)].

The fourth consequence of the model is that the oscillation activity will rise during the inhale and fall at exhale, and that the oscillatory wave rides on a slow wave of background baseline shift phase locked with

the sniff cycles. The oscillation equations

$$\ddot{X}+2\alpha\dot{X}+(A+\alpha^2)X=0 \tag{5.21}$$

have solutions which depend on the matrix $A=H_0G'_y(Y_0)\,W_0G'_x(X_0)$, which in turn depends on the operation point (X_0, Y_0). From (5.7), (X_0, Y_0) depends on the receptor input I as follows:

$$\begin{aligned} dX_0 &\approx(\alpha^2+HW)^{-1}(\alpha dI+d\dot{I}),\\ dY_0 &\approx(\alpha^2+WH)^{-1}(WdI-\alpha H^{-1}d\dot{I}). \end{aligned} \tag{5.22}$$

It turns out that the $d\dot{I}$ terms are negligible except at the initial inhale and exhale instant. Thus the oscillation center (X_0, Y_0) or the baseline shift wave rises and falls with I, or is phase locked with the sniff cycles. Furthermore, the oscillation Eq. (5.21) will have growing oscillation mode only if $\mathrm{Re}(-\alpha\pm i\sqrt{\lambda_k})>0$ for some k, which means that the eigenvalue λ_k of A is large enough. This requires the gain $G'_x(X_0)G'_y(Y_0)$ be high enough to make $A=H_0G'_y(Y_0)W_0G'_x(X_0)$ large. Before inhaling, (X_0, Y_0) is low on the input-output curve and the gain is too small. During the inhale, the increasing receptor input I raises (X_0, Y_0) towards higher gain points. When at some point $\mathrm{Re}(-\alpha\pm i\sqrt{\lambda_k})>0$ is satisfied for some mode k, the oscillation mode will emerge from noise. During the exhale, the receptor input decreases and the process reverses its direction, thus the oscillation decays away.

6 Computations in the Olfactory Bulb

6.1 Information Transmission and Extraction in the Olfactory Bulb

Different odors I give different mean firing rates of the bulb output response. More importantly, since the operation point (X_0, Y_0) also determines the oscillation solutions of (5.21) through matrix $A=H_0G'_y(Y_0)W_0G'_x(X_0)$, different receptor inputs I also give different oscillation pattern outputs indirectly through (X_0, Y_0).

A surge of odor input due to inhalation raises (X_0, Y_0) to a higher gain point $(G'_x(X_0), G'_y(Y_0))$. When there is no or little odor input I_{odor}, the point (X_0, Y_0) is still stable and no high amplitude oscillation burst occurs because oscillation modes are damped. Increasing I_{odor} not only raises the mean activity level, but also slowly changes the oscillation modes by structurally changing the oscillation Eq. (5.21) through matrix A. If (X_0, Y_0) is raised to such an extent that one of the modes can grow with time, the equilibrium point (X_0, Y_0) becomes unstable and this mode emerges with oscillatory bursts. In these cases, different oscillation modes that emerge are indicative of the different odor input patterns which are controlling the system parameters (X_0, Y_0). When (X_0, Y_0) is very low, all modes are damped, and only small amplitude oscillations occur, driven by noise and the weak time variation of the odor input.

The stability change (bifurcation) of the equilibrium point (X_0, Y_0) for the oscillation Eq. (5.21) has been suggested by others (Freeman and Skarda 1985; Baird 1986; Skarda and Freeman 1987) for olfactory processing. Baird (1986) has showed how single or double Hopf bifurcation in one or two oscillators can make stable (non-damping) cycles occur. Baird used excitatory-to-excitatory connections in the mitral cells to ensure the possibility of the stable cycles, which are otherwise impossible in systems with less than three coupled oscillators. Our model shows the multiple (N oscillators) Hopf bifurcations with or without requiring excitatory-to-excitatory connections which are weak or absent in the olfactory bulb (Nicoll 1971; Shepherd 1979).

Our larger system shows the relation between the odor input and the oscillation mode in terms of the eigenvectors and eigenvalues of matrix A. The oscillation modes which emerge from the bulbar activity with odor input can be thought of as the decision states reached for odor information. The bulb output classifies the odor inputs by two stages. First, it fails to oscillate appreciably for weak odors (or some particular stronger odors). The absence of oscillation can be interpreted by higher processing centers as the absence of an odor (Skarda and Freeman 1987). Second, when the odor produces an oscillation, the particular pattern of mitral cell activity is specific to an input pattern and its minor variants, i.e., the pattern of oscillation classifies odors. This is chiefly apparent when the responses of individual mitral cells are studied, and tends to disappear in the EEG average.

High gain alone does not ensure the existence of non-damping modes. A symmetric A will not result in growing modes, as argued in Sect. 5.2. Two examples will illustrate how the bulb selectively responds (or doesn't respond) to certain input patterns. The matrix A in (5.17) might for example have the components

$$H_0=\begin{pmatrix} h & h' & 0 & 0 & & \cdots & & 0 & h' \\ h' & h & h' & 0 & & \cdots & & 0 & 0 \\ 0 & h' & h & h' & 0 & 0 & \cdots & 0 & 0 \\ \vdots & \vdots & & & & \cdots & \ddots & & \vdots \\ h' & 0 & & & \cdots & & 0 & h' & h \end{pmatrix}$$

$$W_0=\begin{pmatrix} w & 0 & 0 & 0 & & \cdots & & 0 & 0 \\ 0 & w & 0 & 0 & & \cdots & & 0 & 0 \\ 0 & 0 & w & 0 & 0 & 0 & \cdots & 0 & 0 \\ \vdots & \vdots & & & & \cdots & \ddots & & \vdots \\ 0 & 0 & & & \cdots & & 0 & 0 & w \end{pmatrix}$$

i.e., each mitral cell gives output to its nearest granule cell neighbor only, while each granule cell connects to three nearest mitral cells. The connections are symmetric and uniform. If the receptor input I and central input I_c are also uniform across the bulb, then the matrix $A = H_0 G_y'(Y_0) W_0 G_x'(X_0)$ will be symmetric, and there will be no growing oscillatory response in the bulb output. Such a bulb however, can respond to some non-uniform inputs I, which induce a non-uniform (X_0, Y_0) and, if g_x and g_y are non-linear, a non-symmetric matrix A. A decision state oscillatory output may be reached if the input I is sufficiently non-uniform, (i.e., the odor selectively excites different mitral cells.)

On the other hand, if

$$H_0 = \begin{pmatrix} h & h' & 0 & 0 & & \dots & & 0 & 0 \\ 0 & h & h' & 0 & & \dots & & 0 & 0 \\ 0 & 0 & h & h' & 0 & 0 & \dots & 0 & 0 \\ \vdots & \vdots & & & & \dots & \ddots & & \vdots \\ h' & 0 & & & \dots & & 0 & 0 & h \end{pmatrix}$$

$$W_0 = \begin{pmatrix} w & w' & 0 & 0 & & \dots & & 0 & 0 \\ 0 & w & w' & 0 & & \dots & & 0 & 0 \\ 0 & 0 & w & w' & 0 & 0 & \dots & 0 & 0 \\ \vdots & \vdots & & & & \dots & \ddots & & \vdots \\ w' & 0 & & & \dots & & 0 & 0 & w \end{pmatrix}$$

the synaptic connection is uniform but non-symmetric across the bulb. If everything else stays the same as in the previous example, matrix A will have the form in (5.19) with uniform receptor input I. A bulb with this connection structure can be responsive to a uniform receptor input pattern I if it is strong enough. These two examples demonstrate that the pattern of the synaptic connections in the bulb determines the input patterns to which the bulb selectively responds.

In the real olfactory bulb, the dendrodendritic connections between the mitral and granule cells are mostly reciprocal, suggesting that $W_0 \approx H_0^T$ (the transpose of H_0) if we ignore other connections and presume roughly equal connection strengths. This implies a near symmetric matrix A for uniform inputs if the synaptic connection structure is approximately uniform across the bulb. But mitral cells also send axon collaterals to the granule cells, suggesting $W_0 \approx H_0^T$ *+extra connections*, which have less reason to be thought symmetric.

6.2 Performance Optimization in the Olfactory Bulb

An active mammalian olfactory system samples the inputs by sniffs, each lasting 200 ms to 1 s in rabbits. The olfactory system should make itself ready for the next sniff which may contain different odor information from the previous sniff. If (X, Y) is the initial deviation of the system from the equilibrium point (X_0, Y_0), then the degree to which the k^{th} oscillation mode gets excited is proportional to $\langle XX_k \rangle$. $X = 0$ corresponds to no excitation of any modes, while a random X corresponds to equal chances of excitation for all the modes. Terminating the oscillation during the exhale leaves only random noise and minimum information contamination in the system and helps the bulb to reach an unbiased decision on the odor information for the next sniff. Furthermore, exhaling also changes the operation point (X_0, Y_0) back to the original value before the inhale (Sect. 5.3), making the system ready for the next sniff.

The initial operation point (X_0, Y_0) before a sniff input should be controlled by the motivation level of the animal. If (X_0, Y_0) is very low initially, a strong input I_{odor} is needed to raise the bias (X_0, Y_0) high enough for an oscillation burst output. Less strong input I_{odor} would be required for an initially higher bias. Since the initial bias (X_0, Y_0) is determined by $I_{\text{background}}$ and the central input I_c by (5.7), it seems likely that the motivation level of the animal will be controlled through inputs from higher centers. Our simulation value for $I_{\text{background}}$ and I_c are set such that the (X_0, Y_0) with $I_{\text{odor}} = 0$ is just below the maximum gain point on the non-linear input-output curves (Sect. 3.2). This corresponds to a motivated state; a small amount of odor input can raise the gain to maximum values. Physiologically, the bulbar oscillatory bursts are observed to occur only in motivated animals (Freeman 1978; Freeman and Schneider 1982). And the experimentally measured gain (defined as the change in the mitral firing rate with respect to the change in EEG amplitude) for bulb neural mass is shown to be higher in the motivated states (Freeman 1979a), which can be achieved by raising $I_{\text{background}}$ through central inputs. Experiments even show the existence of oscillations without odor input with nasal breathing in motivated animals (Freeman and Schneider 1982).

The central input I_c is also likely to participate in other olfactory functions as odor masking or sensitivity enhancing for particular odors (see also Freeman and Schneider 1982). These issues will be studied in a further paper.

7 Discussion

Our model of the olfactory bulb is a simplification of the known anatomy and physiology. The net of the mitral and granule cells simulates a group of coupled non-linear oscillators which are the sources of the rhythmic activities in the bulb. The coupling makes the

oscillation coherent across the whole bulb surface with a single frequency for each sniff but different amplitudes and phases for different mitral cells. The model suggests, in agreement with Freeman and coworkers, that stability change bifurcation is used for the bulbar oscillator system to decide primitively on the relevance of the receptor input information. Different non-damping oscillation modes emerging from the bifurcation are used to distinguish the different odors which are the driving source for the bifurcations. These oscillation modes are approximately thought of as the decision states of the system for the odor information. The coupling between the oscillators implies that information from different parts of the bulb is combined to produce a coherent output oscillation mode, and thus a unitary decision. A succeeding paper will use this basic model to study the ability to discriminate odors and to use input from higher centers to suppress or enhance sensitivity to particular target or masking odors.

Our model bulb encodes the non-oscillatory input into oscillatory "AC" output. Since the oscillation is intrinsic to the bulb, the model amplifies the weak odor input by transforming it to the oscillatory output. Consequently, whether or not an oscillatory mode exists indicates whether an odor is present. With the extra information represented in the oscillation phases of the cells, the bulb emphasizes the differences between different input patterns (Sect. 4). Both the analysis and simulation show that the bulb is selectively sensitive, i.e., non-uniformly sensitive, to different receptor input patterns. This selectivity as well as the motivation level of the animal could also be modulated from higher centers (Sect. 6.2). The information encoding scheme suggests that to extract information from the oscillation amplitudes and phases, we should look at the mitral cells rather than the EEG waves in which the detailed amplitude and phase information tend to be averaged out. Within this model, the information is carried by the detailed pattern of activity of the individual mitral cells; the spatial EEG pattern is an information epiphenomenon. This model does not exclude the possibility that the information be coded in the non-oscillatory slow wave X_0, since as is shown in (5.22), X_0 is determined by the odor input.

The chief behaviors do not depend on the number of cells in the model. The frequencies of the oscillation modes are close to the resonant frequency of a single oscillator in the system, and thus independent of the size of the model. However, since the number of the possible oscillation modes is the same as the mitral cell numbers, the simulated model with a small cell number has few oscillation modes, i.e., the simulated model has less decision states or smaller memory capacity than the real bulb. Therefore the simulated bulb does not respond oscillatorily to most randomly selected input patterns P_{odor}.

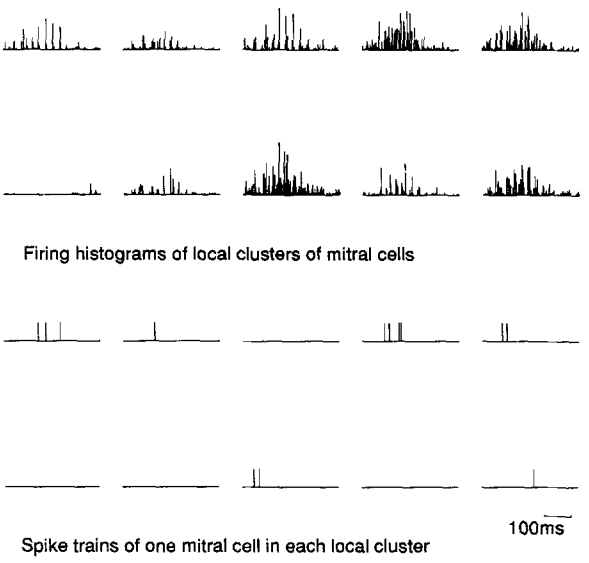

Fig. 8. Simulated bulbar mitral cell response pattern corresponding to Fig. 6A. Each cell is modeled to have discrete action potential firings of maximum rate about 300/s. Each cluster has about 310 mitral cells, and thus a maximum firing rate 93,000/s

Most of the analysis is done for the model bulb without excitatory-to-excitatory and inhibitory-to-inhibitory connections. When those extra connection types are included, the system (5.13) is still a group of coupled non-linear oscillators. This more complicated system is more difficult to analyze, but the solutions will still be oscillation modes which depend on the inputs.

Our model uses a continuous input-output function, instead of discrete spikes that real neurons generate, to describe the neuron outputs. Since the continuous output value is meant to simulate the average of the firing rate of the neurons, unaveraged discrete spike output should chiefly introduce more fluctuations in the system. If the biological system had approximately equivalent close by neurons, then a continuous output would be a good approximation to the group average. Simulation was also done on a model in which each cell in the original model is replaced by a group of cells which generate action potentials rather than continuous valued outputs (Fig. 8). Oscillatory behavior is obvious in the summed spike trains of groups of local cells. But the spike train of a single cell appear very noisy and sparse with barely recognized oscillatory behavior. In the physiological experiment, each mitral cell fires on the average about once in 100 ms (Freeman and Skarda 1985), making it hard to recognize an oscillation with a period of 25 ms in the spike train of a single cell. On the other hand, the

EEG wave is clearly oscillatory since it is from the averaged activities of many local granule cells.

Our simulation has been done on a one-dimensional ring of mitral and granule cells, while the real bulb has cells sitting on two-dimensional segments of a sphere. The dimension of the cell arrangement is not crucial in the model. One simulation was done on a two-dimensional surface of the cells to mimic the real bulb, and the basic oscillation phenomena were very similar to those of the one dimensional rings.

Acknowledgements. This research was supported by ONR contract N00014-87-K-0377.

References

Baird B (1986) Nonlinear dynamics of pattern formation and pattern recognition in rabbit olfactory bulb. Physica 22D:150–175

Bressler S (1987) Relation of olfactory bulb and cortex. I. Spatial variation of bulbo-cortical interdependence. Brain Res 409:285–293

Freeman WJ (1975) Mass action in the nervous system. Academic Press, New York

Freeman WJ (1978) Spatial properties of an EEG event in the olfactory bulb and cortex. Electroencephalogr Clin Neurophysiol 44:586–605

Freeman WJ (1979a) Nonlinear Gain mediating cortical stimulus-response relations. Biol Cybern 33:237–247

Freeman WJ (1979b) Nonlinear dynamics of paleocortex manifested in the olfactory EEG. Biol Cybern 35:21–37

Freeman WJ (1979c) EEG analysis gives model of neuronal template-matching mechanism for sensory search with olfactory bulb. Biol Cybern 35:221–234

Freeman WJ (1980) Use of spatial deconvolution to compensate for distortion of EEG by volume conduction. IEEE Trans Biomed Eng 27:421–429

Freeman WJ, Schneider WS (1982) Changes in spatial patterns of rabbit olfactory EEG with conditioning to odors. Psychophysiology 19:44–56

Freeman WJ, Skarda CA (1985) Spatial EEG patterns, nonlinear dynamics and perception: the Neo-Sherringtonian view. Brain Res Rev 10:147–175

Getchell TV, Shepherd GM (1978) Responses of olfactory receptor cells to step pulses of odour at different concentrations in the salamender. J Physiol 282:521–540

Haberly LB (1985) Neuronal circuitry in olfactory cortex: anatomy and functional implications. Chem Sens 10:219–238

Jahr CE, Nicoll RA (1980) Dendrodendritic inhibition: demonstration with intracellular recording. Science 207:1473–1475

Lancet D (1986) Vertebrate olfactory reception. Ann Rev Neurosci 9:329–355

Lancet D, Greet CA, Kauer JS, Shepherd GM (1982) Mapping of odor-related neuronal activity in the olfactory bulb by high-resolution 2-deoxyglucose autoradiography. Proc Natl Acad Sci USA 79:670–674

Mori K, Kishi K (1982) The morphology and physiology of the granule cells in the rabbit olfactory bulb revealed by intracellular recording and HRP injection. Brain Res 247:129–133

Nicoll RA (1971) Recurrent excitation of secondary olfactory neurons: a possible mechanism for signal amplication. Science 171:824–825

Scott JW (1986) The olfactory bulb and central pathways. Experientia 42:223–232

Shepherd GM (1979) The synaptic organization of the brain. Oxford University Press, New York

Sicard G, Holley A (1984) Receptor cell responses to odorants: similarities and differences among odorants. Brain Res 292:283–296

Skarda CA, Freeman WJ (1987) How brains make chaos in order to make sense of the world. Behav Brain Sci 10:161–195

Received: November 28, 1988

Accepted in revised form: May 3, 1989

Dr. Zhaoping Li
Division of Physics, Mathematics and Astronomy
California Institute of Technology
Pasadena, CA 91125
USA